

## Numerical study of tunneling in a dissipative system

Waldemar Hontscha, Peter Hänggi, Eli Pollak

### Angaben zur Veröffentlichung / Publication details:

Hontscha, Waldemar, Peter Hänggi, and Eli Pollak. 1990. "Numerical study of tunneling in a dissipative system." *Physical Review B* 41 (4): 2210-20.  
<https://doi.org/10.1103/physrevb.41.2210>.

### Nutzungsbedingungen / Terms of use:

licgercopyright

Dieses Dokument wird unter folgenden Bedingungen zur Verfügung gestellt: / This document is made available under these conditions:

**Deutsches Urheberrecht**

Weitere Informationen finden Sie unter: / For more information see:

<https://www.uni-augsburg.de/de/organisation/bibliothek/publizieren-zitieren-archivieren/publiz/>



## Numerical study of tunneling in a dissipative system

Waldemar Hontscha and Peter Hänggi

*Lehrstuhl für Theoretische Physik, Universität Augsburg, Memminger Strasse 6,  
D-8900 Augsburg, Federal Republic of Germany*

Eli Pollak

*Chemical Physics Department, Weizmann Institute of Science, Rehovot 76100, Israel*

(Received 10 August 1989)

Quantum-mechanical resonance energies and their corresponding decay rates (inverse lifetimes) for the metastable system of a cubic potential coupled to a harmonic oscillator are computed numerically via the complex scaling method. This system, which mimics tunneling in dissipative media, is investigated for different barrier heights and a variety of coupling strengths. The large number of computed resonances allows one to calculate thermally averaged decay rates for temperatures up to the crossover temperature. The numerical results are compared to the sudden theory of dissipative tunneling, and rather good agreement is found. The suppression of the rate with increasing dissipation and the thermal enhancement of the rate, as predicted by the instanton method for dissipative tunneling, are also confirmed. When the time scale of the bath oscillator exceeds the time scale of the system, an interesting, counterintuitive observation is that the temperature for the crossover between tunneling and thermally activated escape *increases* with increasing coupling strength. This is in contrast to the usual behavior for ohmiclike dissipative systems. The numerical results in this work can be used as a benchmark to test other theories of dissipative tunneling.

### I. INTRODUCTION

The development of the theory of tunneling in dissipative systems in the past decade has been rapid. The early studies<sup>1,2</sup> concentrated on symmetry breaking at very low temperatures in double-well potentials. The problem itself became well defined through the work of Caldeira and Leggett,<sup>3</sup> who utilized the fact that classical dissipative equations of motion such as generalized Langevin equations (GLE's) may be derived from a Hamiltonian.<sup>4,5</sup> Given a Hamiltonian, one can investigate quantum tunneling rates or any other quantum effect in a dissipative medium. Caldeira and Leggett were mainly interested in the tunneling rate at 0 K. They solved the infinite-dimensional problem by extending the imaginary free energy (Im $F$ ) method of Callan and Coleman.<sup>6</sup> The essence of their solution is a semiclassical steepest-descent evaluation of the free energy, which leads to the instanton<sup>7</sup> as the primary object in the theory. Basically, the instanton is a classical trajectory with infinite period on the upside-down infinite-dimensional potential energy surface. The important qualitative result of their theory was the observation that at 0 K, dissipation will exponentially decrease the tunneling rate relative to the gas-phase rate defined as the tunneling rate without dissipation.

The Im $F$  approach was extended to finite temperatures  $T$  by Grabert, Hänggi, and co-workers.<sup>8-10</sup> Again the central object in their theory is the instanton, which now has a finite period of  $\hbar/k_B T$  ( $k_B$  is Boltzmann's constant). The main result of their study was the observation that heating the bath will cause an exponential power-law enhancement of the rate.<sup>11</sup>

Numerous other papers have been published on the ex-

tension of the semiclassical Im $F$  method to a variety of problems. Other approximate approaches have also been used. Examples are the variational approach to dissipative tunneling in double-well potentials developed by Harris and Silbey<sup>12</sup> and the harmonic tunneling transition state theory approach of Pollak.<sup>13,14</sup> Only recently it has been pointed out that the Im $F$  method is an extension of semiclassical multidimensional transition state theory to dissipative systems.<sup>15</sup>

The major predictions of the theory have been successfully compared with experiment.<sup>16</sup> However, more stringent tests such as *a comparison with numerically exact solutions of metastable model problems is surprisingly lacking*. This does not mean that semiclassical tunneling theories in multidimensional systems have not been tested previously. There is a large body of literature dealing with extensions of the Wentzel-Kramers-Brillouin (WKB) method to multidimensional systems which includes many numerical tests.<sup>17</sup> However, none of the published numerical results can be applied for a direct test of the dissipative tunneling problem as formulated by Caldeira and Leggett. The major purpose of this study is to provide a large body of numerical data which will serve as a benchmark for the testing of approximate solutions.

The model system we will study is that of a cubic oscillator coupled to a single harmonic bath oscillator. Complex numerical eigenvalues of the Hamiltonian are obtained by stabilization of eigenvalues obtained from the complex coordinate method.<sup>18</sup> In Sec. II we define the model system and present numerical results for a range of coupling parameters. Perhaps the most interesting result in this section is the observation that thermal bath excitations can cause an increase of the rate beyond the gas-

phase limit for excited resonance states in the cubic well.

The results obtained in Sec. II are compared with predictions of a sudden theory of tunneling<sup>19</sup> in Sec. III. A detailed analysis of the crossover between tunneling and thermal activation is presented in Sec. IV. We find that the generally accepted definition of a crossover temperature<sup>8–11</sup> between tunneling and activated barrier crossing may not be valid for all memory friction kernels. We end with a discussion of the results, paying special attention to the anomalous behavior of the crossover temperature.

## II. MODEL COMPUTATIONS

### A. The model system

The purpose of this study is to understand the quantum dynamics underlying the classical mechanical GLE of the form

$$M\ddot{q} + \frac{dV}{dq} + M \int_0^t d\tau \gamma(t-\tau)\dot{q}(\tau) = \xi(t). \quad (2.1)$$

Here  $q$  is the system coordinate,  $M$  the mass of the system particle, and  $V(q)$  the system potential chosen as cubic in  $q$ ,

$$V(q) = \frac{1}{2}M\omega_0^2 q^2 - \frac{1}{3}M^{3/2}kq^3. \quad (2.2)$$

$\gamma(t)$  is a time-dependent friction related to the Gaussian random force  $\xi(t)$  through the fluctuation dissipation relation

$$\langle \xi(t)\xi(0) \rangle = k_B T M \gamma(t). \quad (2.3)$$

As demonstrated by Zwanzig,<sup>5</sup> the GLE, Eq. (2.1), may be derived from the Hamiltonian

$$H = \frac{p_q^2}{2M} + V(q) + \sum_{j=1}^N \left[ \frac{p_j^2}{2m_j} + \frac{1}{2}m_j \left[ \omega_j x_j + \frac{C_j}{m_j \omega_j} q \right]^2 \right], \quad (2.4)$$

with the identification

$$\gamma(t) = \frac{1}{M} \sum_{j=1}^N \frac{C_j^2}{m_j \omega_j^2} \cos(\omega_j t). \quad (2.5)$$

One also finds that  $\xi(t)$  is a function of initial conditions which are themselves Gaussian distributed so that Eq. (2.3) holds.

In this paper we limit ourselves to a single bath oscillator with coordinate  $x$  and frequency  $\omega_c$ . This frequency determines a (reduced) memory time

$$\theta \equiv \omega_0 / \omega_c. \quad (2.6)$$

In order to somewhat mimic a continuous ohmic bath with a cutoff frequency  $\omega_c$ , we define a dimensionless coupling parameter  $\alpha$  with the relation

$$\frac{C_1^2}{M m_1 \omega_c^2} \equiv \frac{4}{\pi} \alpha \omega_0^2. \quad (2.7)$$

In anticipation of the sudden theory that is tested in the next section, we note here that around the well ( $q=0$ ) and the barrier ( $q=\omega_0^2/\sqrt{M}k$ ) one can easily find the normal modes by diagonalizing the corresponding force constant matrix.<sup>20</sup> The normal-mode frequencies are designated  $(\lambda_0, \lambda_c)$  around the well, and  $(\lambda_0^\neq, \lambda_c^\neq)$  at the barrier. Here  $\lambda_0^\neq$  denotes the (positive-valued) frequency along the unstable barrier mode. The normal-mode coordinates are rotated with respect to  $q$  and  $x$ . The orthogonal transformation matrix is denoted by  $\underline{U}$  such that

$$\sqrt{M}q = u_{00}\rho + u_{10}y, \quad (2.8)$$

where  $\rho$  and  $y$  are the normal-mode coordinates. In Table I we summarize the numerical values for all relevant normal-mode parameters and potential and coupling parameters used in this paper.

### B. Numerical methods

Resonance energies and lifetimes are computed numerically, using the complex coordinate method. (For some recent reviews and refinements of this method see Ref.

TABLE I. Some relevant normal-mode parameters for the coupled cubic plus harmonic-oscillator system for various values of the dimensionless coupling constant  $\alpha$ .  $\omega_0$  and  $\omega_c$  ( $\lambda_0$  and  $\lambda_c$ ) are the system and bath (normal-mode) frequencies at the well bottom, respectively, where  $\theta \equiv \omega_0/\omega_c = 10$  and  $u_{00}$  is the transformation matrix element according to Eq. (2.8). The corresponding quantities at the barrier top are indexed with  $\neq$ .

$\alpha$	$\lambda_0/\omega_0$	$\lambda_c/\omega_0$	$\lambda_0^\neq/\omega_0$	$\lambda_c^\neq/\omega_0$	$u_{00}^2$	$u_{00}^{\neq 2}$
0.005	1.003 21	0.099 68	0.996 84	0.100 32	0.999 94	0.999 94
0.050	1.031 63	0.096 93	0.967 99	0.103 31	0.999 43	0.999 29
0.100	1.062 99	0.094 14	0.934 94	0.106 96	0.998 98	0.998 37
0.150	1.092 06	0.091 57	0.900 74	0.111 02	0.998 64	0.997 18
0.200	1.121 02	0.089 20	0.865 28	0.115 57	0.998 36	0.995 60
0.300	1.176 75	0.084 98	0.789 97	0.126 59	0.997 98	0.990 59
0.400	1.229 91	0.081 31	0.707 59	0.141 33	0.997 75	0.980 85
0.500	1.280 83	0.078 07	0.616 21	0.162 28	0.997 61	0.959 77
0.600	1.329 77	0.075 20	0.513 75	0.194 65	0.997 54	0.907 61
0.700	1.376 95	0.072 62	0.401 11	0.249 31	0.997 50	0.766 16
0.800	1.422 55	0.070 30	0.294 48	0.339 58	0.997 49	0.478 74

18.) The procedure is based on the analytic continuation of the Hamiltonian via the transformation  $x \rightarrow x \exp(i\varphi_x)$ ,  $q \rightarrow q \exp(i\varphi_q)$ , where in general,  $\varphi_x$  and  $\varphi_q$  may be complex. The theory, relating a complex eigenvalue of this Hamiltonian,  $E - i\hbar\Gamma/2$ , to the resonance energy  $E$  and (inverse) lifetime  $\Gamma$  in a metastable potential, is well understood.

In principle, the complex eigenvalues are independent of the rotating angle. In practice, due to finite basis set limitations, one determines the eigenvalues via the stabilization method.<sup>18</sup> If the basis set is sufficiently large, then there exists a range of angles over which the eigenvalues remain practically constant.

In practice we used two different harmonic-oscillator basis sets with frequencies set either to the normal-mode frequencies at the well ( $\lambda_0, \lambda_c$ ) or to the “bare” frequencies ( $\omega_0, \omega_c$ ). A typical basis set used was  $n_q=40$  ( $n_\rho=40$ ) states for the system, whereas the number of states in the oscillator mode ( $y$  or  $x$ ) was variable; this is inherent to the method of matrix continued fractions<sup>21</sup> used to compute the resonances. Typical stabilization graphs for the imaginary parts of the eigenvalues are shown in Figs. 1(a) and 1(b), the real parts stabilized (to more than 10 digits) over an even wider range of the scaling angle. It turned out to be sufficient to scale via the angle  $\varphi_q$  keeping the angle  $\varphi_x$  constant at  $\varphi_x=0$ . Generally, stabilization, with our choice of a harmonic basis set, was easy to achieve, provided that the reduced tunneling rates ( $\Gamma/\omega_0$ ) did not become smaller than  $\sim 10^{-11}$ , and that, in particular in view of convergence of higher excited states, the coupling  $\alpha$  was not too strong. For very small tunneling rates, the harmonic-oscillator basis used does not extend far enough out into the tunneling region. This fact and the unavoidable numerical finite precision arithmetic limited our study to a barrier whose maximal reduced height  $V^\ddagger/\hbar\omega_0=3$  and a maximal coupling strength of  $\alpha=0.2$  or  $V^\ddagger/\hbar\omega_0=1$  at  $\alpha=0.8$ . Even with these limitations, the numerical effort is extensive.

### C. Numerical results

As a check, we first compared our results for the uncoupled cubic oscillator with the results obtained in Ref. 22, and in addition, to the instanton results of Refs. 23 and 24. This comparison is summarized in Table II. It is interesting to point out that even for a one-dimensional system the standard instanton approximation<sup>6</sup> can be less precise than the standard WKB expression.<sup>7</sup> The instanton (INS) rate  $\Gamma^{\text{INS}}$  is given by the expression<sup>3,23,24</sup>

$$\begin{aligned} \Gamma^{\text{INS}} &= A_0 \exp(-B_0), \\ A_0 &= \frac{\omega_0}{(2\pi)^{1/2}} (60B_0)^{1/2}, \\ B_0 &= \frac{6}{5} \frac{\omega_0^5}{\hbar k^2}. \end{aligned} \quad (2.9)$$

The WKB rate  $\Gamma_n^{\text{WKB}}$  from the  $n$ th excited state is determined as

$$\Gamma_n^{\text{WKB}} = \frac{1}{\tau(E_n)} \exp\left[-\frac{W_n}{\hbar}\right], \quad (2.10)$$

TABLE II. Resonance energies and the corresponding decay rates for a one-dimensional cubic potential with reduced barrier height  $V^\ddagger/\hbar\omega_0$  of value 1 and 3, respectively, computed by the method of complex scaling. Comparison is made with the predictions of simple WKB theory and the instanton formalism.  $\Gamma_{\text{CS}}^{\text{WKB}}$  and  $\Gamma_{\text{BSQ}}^{\text{WKB}}$  are the WKB rates based on the resonance energies found by complex scaling (CS) and by using the Bohr-Sommerfeld quantization (BSQ), respectively.  $n$  denotes the excitation level in the cubic well.

$V^\ddagger/\hbar\omega_0$	$n$	Complex scaling			WKB		Instanton $\Gamma^{\text{INS}}/\omega_0$
		$\text{Re}E_{\text{CS}}/\hbar\omega_0$	$\Gamma_{\text{CS}}/\omega_0$	$\Gamma_{\text{CS}}^{\text{WKB}}/\hbar\omega_0$	$\text{Re}E_{\text{BSQ}}/\hbar\omega_0$	$\Gamma_{\text{BSQ}}^{\text{WKB}}/\hbar\omega_0$	
1	0	0.465 138 76 484(5)	$4.540\,033\,5(1) \times 10^{-3}$	$4.330\,888\,22 \times 10^{-3}$	$0.479\,280\,806\,621$	$4.761\,506\,44 \times 10^{-3}$	$6.190\,584\,69 \times 10^{-3}$
3	0	0.490 867 406 24(2)	$5.563(2) \times 10^{-9}$	$5.1428 \times 10^{-9}$	$0.493\,911\,528\,930$	$5.2678 \times 10^{-9}$	$5.9766 \times 10^{-9}$
3	1	1.436 230 250 0(5)	$5.1827(5) \times 10^{-6}$	$5.031\,28 \times 10^{-6}$	$1.439\,775\,080\,62$	$5.155\,04 \times 10^{-6}$	
3	2	2.304 595 845(9)	$1.540\,303(9) \times 10^{-3}$	$1.539\,432\,3 \times 10^{-3}$	$2.309\,217\,910\,4$	$1.585\,181\,8 \times 10^{-3}$	

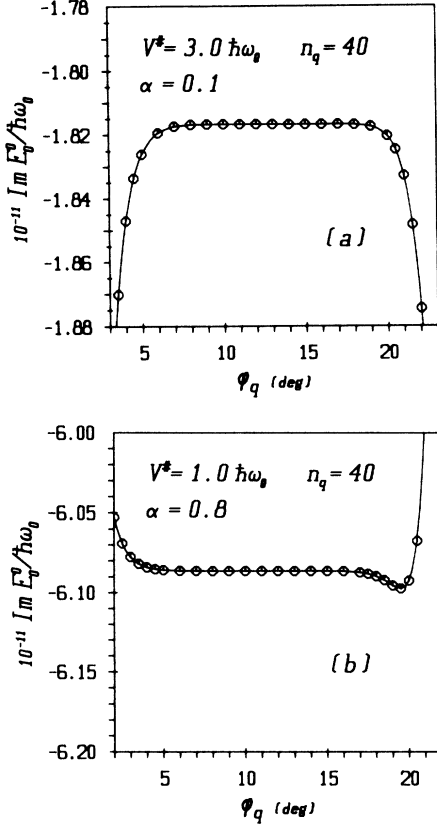


FIG. 1. Typical stabilization graphs for the imaginary part of the lowest resonance state vs the scaling angle  $\varphi_q$  ( $\varphi_x=0$ ) in the cubic well coupled to a harmonic oscillator. The reduced barrier heights and coupling strengths are  $V^\#/\hbar\omega_0=3.0$ ,  $\alpha=0.1$  [part (a)] and  $V^\#/\hbar\omega_0=1$ ,  $\alpha=0.8$  [part (b)], respectively. The number of basis states in the system coordinate was  $n_q=40$ .

where  $\tau(E_n)$  is the period for one oscillation in the well at the semiclassical energy  $E_n$  determined by the Bohr-Sommerfeld quantization rule and  $W_n$  is the abbreviated action through the barrier at the same energy.

Note that with increasing barrier height the instanton expression becomes more accurate than the WKB result, but for a low barrier ( $V^\#/\hbar\omega_0=1$ ) the WKB method is superior (see Table II). Presumably this is a reflection of the fact that for a low barrier the ground state has substantial anharmonic contributions. The harmonic approximation for motion in the well is an essential part of the instanton method. It will be of interest to understand whether this difference will remain when the cubic oscillator is coupled to a bath. This consideration motivated a detailed numerical study of the coupled oscillator model at the same reduced barrier heights.

All results presented for the coupled oscillator model [cf. Eq. (2.6)] are with reduced memory time  $\theta=10$ , in anticipation of the sudden approximation to be tested in the next section and in view of the fact, that for ohmic-like dissipation, the low-frequency bath modes are the “source” of the interesting physics. In Table III, we tabulate the converged complex eigenvalues for reduced

TABLE III. Some complex resonance energies for the coupled cubic plus harmonic oscillator system at coupling strength  $\alpha=0.5$  and a reduced barrier height  $V^\#/\hbar\omega_0=1$ .  $n(k)$  denotes the excitation level in the system (oscillator) mode. The ratio of system and bath frequency is  $\theta\equiv\omega_0/\omega_c=10$ .

$n$	$k$	$\text{Re}E_n^k/\hbar\omega_0$	$-\text{Im}E_n^k/\hbar\omega_0$
0	0	0.661 541 373(7)	$3.008(5)\times 10^{-7}$
0	1	0.735 502 771(5)	$3.866(9)\times 10^{-6}$
0	2	0.808 765 908(7)	$2.780(2)\times 10^{-5}$
1	0	1.848 339 17(0)	$4.450 33(8)\times 10^{-2}$
1	1	1.915 565 83(8)	$6.623 01(9)\times 10^{-2}$
1	2	1.985 280 17(1)	$8.672 39(9)\times 10^{-2}$
2	0	2.806 469(6)	$2.479 70(8)\times 10^{-1}$
2	1	2.890 673(1)	$2.747 31(1)\times 10^{-1}$
2	2	2.974 188(8)	$3.004 86(7)\times 10^{-1}$

barrier height of unity and  $\alpha=0.5$ . Comparison with Table II shows that the ground-state rates have decreased, as a result of the coupling, by four orders of magnitude. At  $\alpha=0.5$  one can still assign each one of the resonance states according to  $H_0$ —the uncoupled normal-mode harmonic-oscillator Hamiltonian. Thus  $E_n^k$  and  $\Gamma_n^k$  are the energies and rates, respectively, for  $n$  excitations in the system mode ( $\rho$ ) and  $k$  excitations in the bath mode ( $y$ ). It is interesting to note that bath excitations cause a strong enhancement of the rate. This is shown graphically for the  $V^\#/\hbar\omega_0=3$  case in Figs. 2(a)–2(c). Evidently, bath excitations reduce the effective barrier height for tunneling, enhancing the rate, in qualitative agreement with the instanton-based predictions of the thermal enhancement of the rate.

Since assignment of each state is still possible, one may define thermal tunneling rates  $\Gamma_n(T)$  for each system resonance state separately:

$$\Gamma_n(t) \equiv \sum_{k=0}^{\infty} \exp(-\beta E_n^k) \Gamma_n^k / \sum_{k=0}^{\infty} \exp(-\beta E_n^k), \quad (2.11)$$

where  $\beta=1/k_B T$ . In Table IV we tabulate these thermal rates for a variety of parameters. Also given in the table are the thermally averaged rates. Denoting the  $n$ th system state partition function as

$$Z_n(T) \equiv \sum_{k=0}^{\infty} \exp[-\beta(E_n^k - E_n^0)], \quad (2.12)$$

one finds that the thermally averaged canonical rate may be expressed as

$$\Gamma(T) \equiv \frac{\sum_{n,k=0}^{\infty} \exp(-\beta E_n^k) \Gamma_n^k}{\sum_{n,k=0}^{\infty} \exp(-\beta E_n^k)} = \frac{\sum_{n=0}^{\infty} \exp(-\beta E_n^0) Z_n(T) \Gamma_n(T)}{\sum_{n=0}^{\infty} \exp(-\beta E_n^0) Z_n(T)}. \quad (2.13)$$

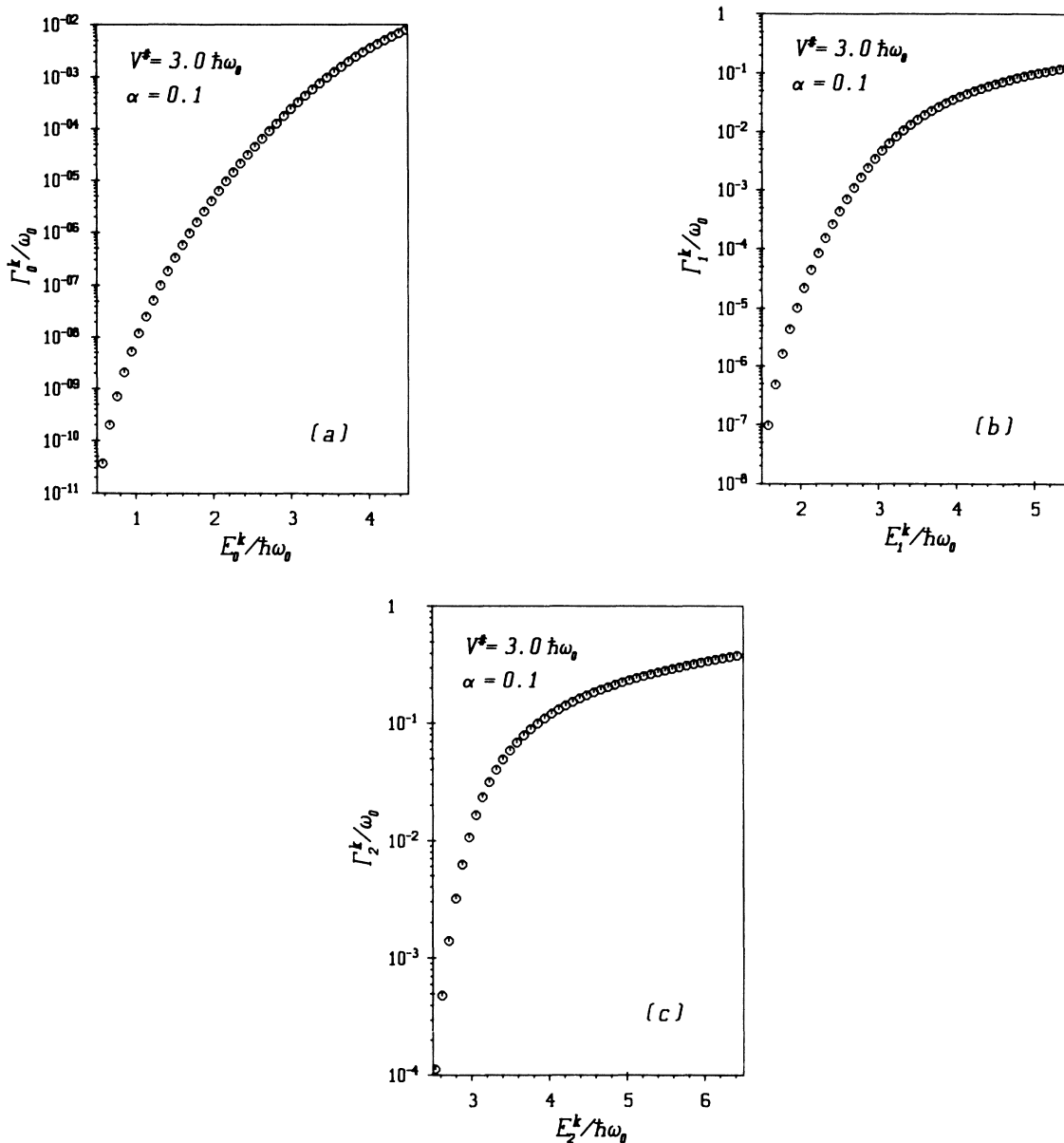


FIG. 2. (a)–(c) Decay widths  $\Gamma_n^k$  vs their corresponding resonance energies  $E_n^k$  for the ground ( $n=0$ ), first ( $n=1$ ), and second ( $n=2$ ) excited state, respectively, in the cubic oscillator mode. Note the strong enhancement of the decay rates due to the excitation of the bath oscillator (superscript  $k$ ). The reduced barrier height  $V^\ddagger/\hbar\omega_0=3$ , the ratio of the well frequency  $\omega_0$  to the harmonic-oscillator frequency  $\omega_c$  is  $\theta \equiv \omega_0/\omega_c = 10$ , and the coupling strength  $\alpha=0.1$ .

Convergence of the numerical eigenvalues ( $E_n^k, \Gamma_n^k$ ) is good only for states whose (reduced) tunneling rates ( $\Gamma_n^k/\omega_0$ ) are  $\sim 0.4$  or less. This implies that the thermal rates in (2.11)–(2.13) will be converged numerically as long as the decay is solely governed by tunneling. Therefore, we computed thermal decay rates only for temperatures below  $T_0$ , defined as

$$k_B T_0 \equiv \hbar\omega_0^\ddagger/2\pi \quad (2.14)$$

(for a cubic potential  $\omega_0^\ddagger = \omega_0$ ).

When  $\alpha=0$ ,  $T_0$  is the crossover temperature between tunneling and thermal activation (see also Sec. IV). It is

interesting to note from Table IV that for all temperatures reported, the thermally averaged canonical rate [Eq. (2.13)] for  $\alpha>0$  is always less than the analogous thermally averaged ( $\alpha=0$ ) gas-phase rate. This is in full agreement with the instanton-based prediction that for temperatures below crossover, dissipation always decreases the tunneling rate. The results are also in agreement with the prediction based on a sudden theory,<sup>19</sup> that for excited resonance states, the thermally averaged rate with dissipation [Eq. (2.13)] may exceed the gas-phase rate even below crossover. A detailed comparison with the sudden approximation is presented in the next section.

### III. THE SUDDEN APPROXIMATION

It has been noted previously,<sup>13a,19,25</sup> that the enhancement of the dissipative tunneling rate at low temperatures comes as a result of the excitation of the low-frequency modes. Since almost by definition these modes move slowly relative to the system motion, it is natural to try to understand their effect, using a frozen bath approximation, also known in the Chemical Physics literature as the sudden approximation. A sudden approximation for tunneling in dissipative systems has been recently formulated;<sup>19</sup> here we test its accuracy on the numerical results presented in the preceding section. The condition for validity of this approximation is that  $\theta \equiv \omega_0/\omega_c \gg 1$ . Therefore the model chosen was estimated at  $\theta = 10$ .

The starting point is the Hamiltonian [Eq. (2.4)] but written in the normal-mode coordinates at the well  $(\rho, y)$ . (In principle one can also derive a sudden approximation using the normal-mode expansion around the barrier. This gives an identical result in the weak-coupling limit. In the strong-coupling limit though, one can show<sup>19</sup> that the sudden limit is valid only if one uses the normal-mode analysis around the well.) Since the coordinate  $y$  is a constant, the conjugate momentum  $p_y = 0$  and the Hamiltonian may be brought to a convenient form, by choosing the following scaling: Time is scaled by  $1/\lambda_0$ , energy by  $\lambda_0^6/k^2 u_{00}^6$ , and the coordinates  $u_{00}\rho$ ,  $u_{10}y$  by  $ku_{00}^2/\lambda_0^2$ . This leaves us with the reduced cubic sudden Hamiltonian<sup>19</sup>

$$h = \frac{1}{2}p'^2 + \frac{1}{2}(1-4v')^{1/2}\rho'^2 - \frac{1}{3}\rho'^3, \quad (3.1)$$

where  $\rho'$  and  $v'$  are the reduced coordinates and  $p$  is the momentum conjugate to  $\rho'$ . The effect of the bath enters through the variance of the variable  $v'$ , which is a Gaussian random variable stemming from the harmonic nature of the bath mode.

When the bath coordinate is in thermal equilibrium, then  $\langle v' \rangle = 0$  and the temperature-dependent variance is

$$\langle v'^2 \rangle = \frac{\hbar}{2} \frac{k^2 u_{00}^4}{\lambda_0^4} \frac{u_{10}^2}{\lambda_1} \coth(\hbar\beta\lambda_1/2). \quad (3.2)$$

For each frozen bath value  $v'$ , the Hamiltonian is a one degree of freedom cubic Hamiltonian for which the instanton expression for tunneling from the ground state is given by Eq. (2.9) with suitable scaling. Thus

$$\Gamma^{\text{INS}}(v') \equiv A_0(v') \exp[-B_0(v')], \quad (3.3)$$

and one finds

$$A_0(v') = A_0 \left[ \frac{\lambda_0}{u_{00}\omega_0} (1-4v')^{1/4} \right]^{7/2} u_{00}^{1/2}, \quad (3.4)$$

$$B_0(v') = B_0 \left[ \frac{\lambda_0}{u_{00}\omega_0} (1-4v')^{1/4} \right]^5 / u_{00}, \quad (3.5)$$

where  $A_0$ , and  $B_0$  are already defined in Eq. (2.9).

The thermal rate is obtained by averaging the frozen bath rate over the  $v'$  distribution

TABLE IV. Thermally averaged rates of decay out of a cubic potential with reduced barrier height  $V^\#/\hbar\omega_0 = 3$ , which is coupled to a single harmonic oscillator. The ratio  $\theta$  of cubic well frequency  $\omega_0$  and the oscillator frequency  $\omega_c$  is  $\theta = 10$ ,  $\alpha$  is the coupling strength [Eq. (2.7)], and  $T_0$  the uncoupled crossover temperature [Eq. (2.14)].  $\Gamma$  denotes the canonically averaged thermal rate and  $\Gamma_n$  ( $n = 0, 1, 2$ ) means the thermally averaged rate from the  $n$ th excitation of the system mode. For the computation of the full rate  $\Gamma$  the third excitation level in the system mode was also taken into account.

$T/T_0$	Thermally averaged decay rates									
	$\alpha = 0.05$			$\alpha = 0.005$			$\alpha = 0.0$			
	$\Gamma_0/\omega_0$	$\Gamma_1/\omega_0$	$\Gamma_2/\omega_0$	$\Gamma_0/\omega_0$	$\Gamma_1/\omega_0$	$\Gamma_2/\omega_0$	$\Gamma_0/\omega_0$	$\Gamma_1/\omega_0$	$\Gamma_2/\omega_0$	$\Gamma/\omega_0$
0.1	$3.68 \times 10^{-11}$	$9.79 \times 10^{-8}$	$1.14 \times 10^{-4}$	$3.68 \times 10^{-11}$	$7.83 \times 10^{-7}$	$4.67 \times 10^{-4}$	$4.95 \times 10^{-10}$	$4.40 \times 10^{-9}$	$4.33 \times 10^{-6}$	$1.38 \times 10^{-3}$
0.2	$4.66 \times 10^{-11}$	$1.22 \times 10^{-7}$	$1.39 \times 10^{-4}$	$4.66 \times 10^{-11}$	$8.58 \times 10^{-7}$	$5.05 \times 10^{-4}$	$5.47 \times 10^{-10}$	$4.44 \times 10^{-9}$	$4.36 \times 10^{-6}$	$1.39 \times 10^{-3}$
0.3	$7.49 \times 10^{-11}$	$1.88 \times 10^{-7}$	$2.03 \times 10^{-4}$	$7.49 \times 10^{-11}$	$1.04 \times 10^{-6}$	$5.88 \times 10^{-4}$	$6.76 \times 10^{-10}$	$4.53 \times 10^{-9}$	$4.43 \times 10^{-6}$	$1.41 \times 10^{-3}$
0.4	$1.34 \times 10^{-10}$	$3.18 \times 10^{-7}$	$3.10 \times 10^{-4}$	$1.34 \times 10^{-10}$	$1.31 \times 10^{-6}$	$7.04 \times 10^{-4}$	$8.81 \times 10^{-10}$	$4.64 \times 10^{-9}$	$4.53 \times 10^{-6}$	$1.43 \times 10^{-3}$
0.5	$2.49 \times 10^{-10}$	$5.55 \times 10^{-7}$	$4.69 \times 10^{-4}$	$2.51 \times 10^{-10}$	$1.69 \times 10^{-6}$	$8.51 \times 10^{-4}$	$1.18 \times 10^{-9}$	$4.76 \times 10^{-9}$	$4.63 \times 10^{-6}$	$1.45 \times 10^{-3}$
0.6	$4.71 \times 10^{-10}$	$9.71 \times 10^{-7}$	$6.86 \times 10^{-4}$	$4.96 \times 10^{-10}$	$2.19 \times 10^{-6}$	$1.03 \times 10^{-3}$	$1.66 \times 10^{-9}$	$4.90 \times 10^{-9}$	$4.75 \times 10^{-6}$	$1.48 \times 10^{-3}$
0.7	$8.91 \times 10^{-10}$	$1.68 \times 10^{-6}$	$9.67 \times 10^{-4}$	$1.10 \times 10^{-9}$	$2.85 \times 10^{-6}$	$1.23 \times 10^{-3}$	$2.64 \times 10^{-9}$	$5.04 \times 10^{-9}$	$4.87 \times 10^{-6}$	$1.51 \times 10^{-3}$
0.8	$1.67 \times 10^{-9}$	$2.86 \times 10^{-6}$	$1.31 \times 10^{-3}$	$2.98 \times 10^{-9}$	$3.71 \times 10^{-6}$	$1.46 \times 10^{-3}$	$5.21 \times 10^{-9}$	$5.19 \times 10^{-9}$	$4.99 \times 10^{-6}$	$1.53 \times 10^{-3}$
0.9	$3.09 \times 10^{-9}$	$4.73 \times 10^{-6}$	$1.73 \times 10^{-3}$	$9.46 \times 10^{-9}$	$4.81 \times 10^{-6}$	$1.72 \times 10^{-3}$	$1.31 \times 10^{-8}$	$5.35 \times 10^{-9}$	$5.12 \times 10^{-6}$	$1.56 \times 10^{-3}$
1.0	$5.65 \times 10^{-9}$	$7.60 \times 10^{-6}$	$2.21 \times 10^{-3}$		$6.21 \times 10^{-6}$	$2.00 \times 10^{-3}$		$5.52 \times 10^{-9}$	$5.26 \times 10^{-6}$	$1.59 \times 10^{-3}$
										$5.56 \times 10^{-9}$
										$5.56 \times 10^{-9}$
										$5.56 \times 10^{-9}$
										$5.57 \times 10^{-9}$
										$5.60 \times 10^{-9}$
										$5.83 \times 10^{-9}$
										$6.77 \times 10^{-9}$
										$9.84 \times 10^{-9}$
										$1.84 \times 10^{-8}$

$$\Gamma^{\text{INS}}(T) = (2\pi \langle v'^2 \rangle)^{-1/2} \times \int_{-\infty}^{\infty} dv' \exp \left[ -\frac{v'^2}{2 \langle v'^2 \rangle} \right] \Gamma^{\text{INS}}(v'). \quad (3.6)$$

The integral may be estimated using a steepest-descent approximation (as long as  $T < T_0$ ); the details are given in Ref. 19. The steepest-descent approximation was tested against an exact numerical integration for all parameters studied in this paper, and agreement between the two was excellent.

In the weak-coupling limit  $\alpha \ll 1$ , one can obtain the following explicit results for the normal-mode parameters:

$$\lambda_0^2 \simeq \omega_0^2 \left[ 1 + \frac{4}{\pi} \alpha \right], \quad \lambda_c^2 \simeq \omega_c^2 \left[ 1 - \frac{4}{\pi} \alpha \right], \quad (3.7)$$

$$u_{00}^2 \simeq 1 - \frac{4}{\pi} \frac{\alpha}{\theta^2}, \quad u_{10}^2 \simeq \frac{4}{\pi} \frac{\alpha}{\theta^2}. \quad (3.8)$$

The fact that the coupling enhances the difference between the system and bath frequency is a general result for any coupling and any number of bath modes as long as the cutoff frequency  $\omega_c$  is less than  $\omega_0$ . This implies, that at least for the system studied in Sec. II, coupling should enhance the range of validity of the sudden approximation.

In the weak-coupling limit one can then obtain analytic estimates for the rate. One finds that

$$\langle v'^2 \rangle \simeq \frac{6}{5} \frac{B_0 \alpha}{\pi \theta} \coth(\hbar \beta \omega_c / 2). \quad (3.9)$$

Defining a cutoff temperature  $T_c$

$$k_B T_c = \frac{\hbar \omega_c}{2\pi}, \quad (3.10)$$

it is easy to see that for  $T \ll T_c$ ,  $\langle v'^2 \rangle$  becomes essentially temperature independent, while for higher temperatures

$$\langle v'^2 \rangle \simeq \frac{6}{5\pi^2} B_0 \alpha \frac{T}{T_0}, \quad T_c \ll T \leq T_0. \quad (3.11)$$

As a result, for  $T=0$  one finds in the weak-coupling limit

$$\Gamma^{\text{INS}}(0) \simeq A_0 \left[ 1 + \frac{7}{\pi} \alpha \right] \times \exp \left\{ -B_0 \left[ 1 + \frac{10\alpha}{\pi} \left[ 1 - \frac{3}{\theta} \right] + O(\alpha^2) \right] \right\}. \quad (3.12)$$

For temperatures greater than  $T_c$  the rate is

$$\Gamma^{\text{INS}}(T) \simeq A_0 \left[ 1 + \frac{7}{\pi} \alpha \right] \times \exp \left\{ -B_0 \left[ 1 + \frac{10\alpha}{\pi} \left[ 1 - \frac{3}{\pi} \frac{T}{T_0} \right] \right] \right\}. \quad (3.13)$$

The linear dependence of the exponential on the tempera-

ture is also predicted within the sudden theory<sup>19</sup> for a continuous distribution of mode frequencies with a cutoff frequency  $\omega_c$ . This is due to the fact that for temperatures  $T > T_c$  the bath can be treated classically mechanically (quantum bath effects are no longer important). It is also interesting to note that for all  $T < T_0$  this result explicitly demonstrates that the ‘‘bath’’ decreases the ground-state tunneling rate with respect to the gas phase.

The effect of coupling on the  $T=0$  K rate is shown in Figs. 3(a) and 3(b), together with a comparison with the sudden theory for a low and a high barrier. As noted in the preceding section, for  $V^\ddagger/\hbar\omega_0=1$ , at zero coupling, the instanton estimate is not very accurate. Here we see

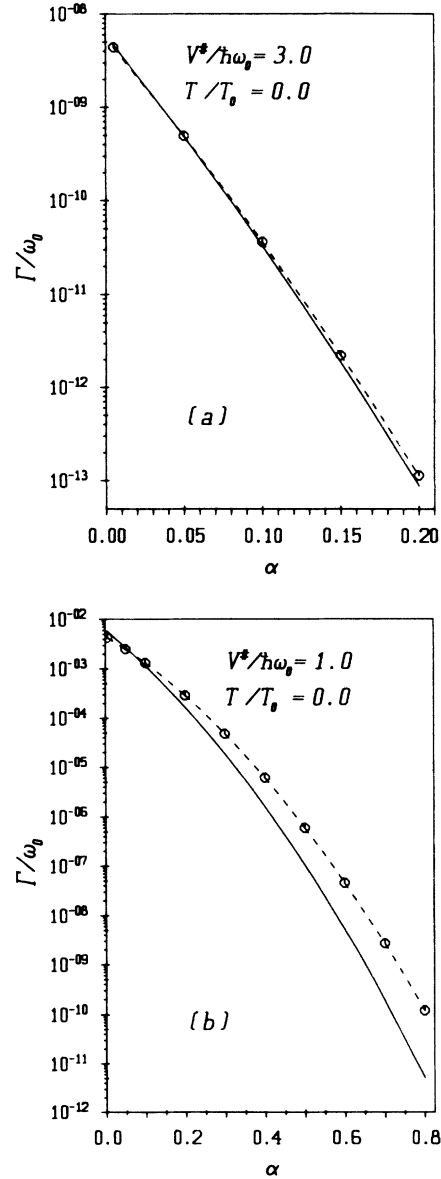


FIG. 3. Dependence on the coupling constant  $\alpha$  of the zero-temperature decay rate  $\Gamma$  out of the coupled cubic plus harmonic system for reduced barrier height  $V^\ddagger/\hbar\omega_0=3$  [part (a)] and  $V^\ddagger/\hbar\omega_0=1$  [part (b)], respectively. The dashed curves interpolate the values computed by the method of complex scaling and the full curves are the prediction of the sudden theory.

TABLE V. We display the thermal decay rates from the ground state of a metastable potential with reduced barrier height  $V^\ddagger/\hbar\omega_0=3$  coupled to a harmonic oscillator, as predicted by the sudden theory in function of temperature for various coupling strengths.

$T/T_0$	$\Gamma_0(T)/\omega_0$			
	$\alpha=0.05$	$\alpha=0.10$	$\alpha=0.15$	$\alpha=0.20$
0.0	$4.842 \times 10^{-10}$	$3.291 \times 10^{-11}$	$1.867 \times 10^{-12}$	$8.807 \times 10^{-14}$
0.1	$4.865 \times 10^{-10}$	$3.330 \times 10^{-11}$	$1.909 \times 10^{-12}$	$9.132 \times 10^{-14}$
0.2	$5.370 \times 10^{-10}$	$4.184 \times 10^{-11}$	$2.825 \times 10^{-12}$	$1.651 \times 10^{-13}$
0.3	$6.611 \times 10^{-10}$	$6.642 \times 10^{-11}$	$6.064 \times 10^{-12}$	$5.034 \times 10^{-13}$
0.4	$8.576 \times 10^{-10}$	$1.168 \times 10^{-10}$	$1.511 \times 10^{-11}$	$1.855 \times 10^{-12}$
0.5	$1.139 \times 10^{-9}$	$2.138 \times 10^{-10}$	$3.945 \times 10^{-11}$	$7.127 \times 10^{-12}$
0.6	$1.528 \times 10^{-9}$	$3.961 \times 10^{-10}$	$1.032 \times 10^{-10}$	$2.680 \times 10^{-11}$
0.7	$2.060 \times 10^{-9}$	$7.328 \times 10^{-10}$	$2.649 \times 10^{-10}$	$9.579 \times 10^{-11}$
0.8	$2.779 \times 10^{-9}$	$1.344 \times 10^{-9}$	$6.596 \times 10^{-10}$	$3.206 \times 10^{-10}$
0.9	$3.747 \times 10^{-9}$	$2.436 \times 10^{-9}$	$1.583 \times 10^{-9}$	$9.972 \times 10^{-10}$
1.0	$5.041 \times 10^{-9}$	$4.348 \times 10^{-9}$	$3.651 \times 10^{-9}$	$2.873 \times 10^{-9}$

that with coupling, the sudden theory based on the one-dimensional instanton estimate is only semiquantitative. On the other hand, for the higher barrier, where the instanton estimate with zero coupling is more accurate, we find that the sudden theory with damping is rather good. Temperature effects are shown in Figs. 4(a) and 4(b). Here we find, that even when the  $T=0$  K rate for the low barrier ( $V^\ddagger/\hbar\omega_0=1$ ) is not precisely predicted from the sudden theory, the relative effect is qualitatively accounted for by the sudden approximation. For the high barrier, the temperature enhancement of the rate is described quite accurately by the sudden theory. Numerical values for the thermal rate predicted by sudden theory for decay from the ground state of the metastable potential with reduced barrier height  $V^\ddagger/\hbar\omega_0=3$  at vari-

ous coupling strengths are given in Table V, for the purpose of eventual comparison with other theories for dissipative tunneling.

#### IV. THE CROSSOVER TEMPERATURE

At very low temperatures it is clear that the rate of escape is dominated by tunneling. At  $T=0$  K, the classical particle cannot escape, while quantum mechanically there is always a finite tunneling rate. At high temperatures, the particle gains enough energy to cross the barrier and the rate becomes dominated by classical thermal activation. Without dissipation one finds that the crossover temperature is given by Eq. (2.14). A simple way to obtain this estimate is via a harmonic tunneling approximation. Assuming that the rate is

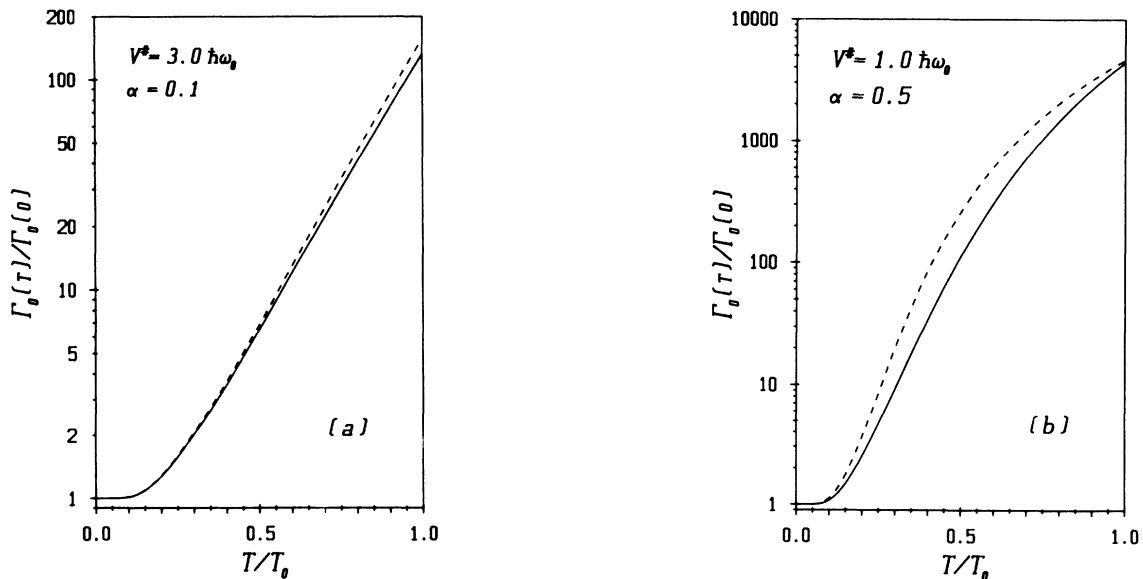


FIG. 4. Temperature enhancement of the decay rate from the ground state of the cubic oscillator mode  $\Gamma_0(T)/\Gamma_0(0)$  for  $V^\ddagger/\hbar\omega_0=3$ ,  $\alpha=0.1$  [part (a)] and  $V^\ddagger/\hbar\omega_0=1$ ,  $\alpha=0.5$  [part (b)], respectively. The dashed curves represent the behavior found from complex scaling data and the solid curve is the enhancement predicted by the sudden theory.

$$\Gamma(E) \propto \exp \left[ -\frac{2\pi}{\hbar\omega^\ddagger} (V^\ddagger - E) \right], \quad (4.1)$$

and equating it with the Boltzmann factor  $e^{-\beta E}$ , one finds that for  $T < T_0$  the weighted rate  $e^{-\beta E}\Gamma(E)$  decreases as  $E$  increases (indicating the dominance of tunneling), while for  $T > T_0$  the weighted rate increases as  $E$  increases, indicating the dominance of thermal activation. The same estimate may be applied to tunneling in the presence of dissipation; the only change is that now the tunneling is dominated by the normal-mode barrier so that  $\omega^\ddagger$  in Eq. (4.1) is replaced by  $\lambda^\ddagger$ —the normal-mode barrier frequency. This leads to the estimate of an  $\alpha$ -dependent crossover temperature  $T_\alpha$ ,

$$k_B T_\alpha = \hbar\lambda_0^\ddagger / 2\pi, \quad (4.2)$$

derived originally by Hänggi *et al.*<sup>26</sup> using a more rigorous instanton analysis.

One might question the validity of this estimate, since seemingly it is dependent on a harmonic approximation. In fact, around the crossover temperature, provided that  $V^\ddagger/\hbar\omega^\ddagger \gg 1$ , the escape rate is dominated by the dynamics whose energy is at the barrier height. As a result the harmonic approximation is not only justified, but arises naturally from the instanton-based estimates of the rate.

As already mentioned, our numerical stabilization computation yields converged rates only when tunneling dominates the escape. This implies that a converged thermal rate  $\Gamma_n(T)$  [cf. Eq. (2.11)] from the  $n$ th resonance state in the normal mode well can be obtained only if  $E_n^0 \lesssim V^\ddagger$ . It is, therefore, not possible to obtain the converged canonical rate, Eq. (2.13), for high temperatures. However, it is possible to study the crossover by inspecting the weighted energy dependence

$$f_n(T) \equiv \exp(-\beta E_n^0) Z_n(T) \Gamma_n(T) \quad (4.3)$$

of the rate as a function of  $n$ . In Fig. 5 we show the normalized weights

$$P_n(T) \equiv f_n(T)/f_0(T) \quad (4.4)$$

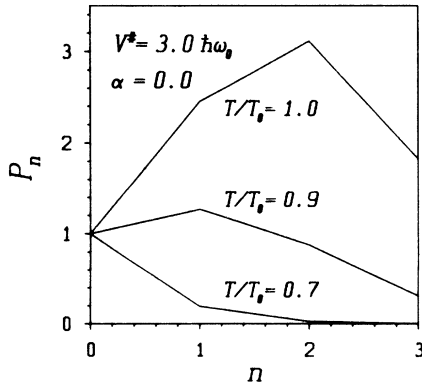


FIG. 5. Normalized thermal weights  $P_n$  [see Eqs. (2.11)–(2.13) and (4.3)–(4.4)], i.e., the relative contributions to the thermal rate, of the ground, first-, second-, and third-excited state ( $n=0,1,2,3$ ) in a one-dimensional cubic potential of reduced height  $V^\ddagger/\hbar\omega_0=3$  for three different temperatures.

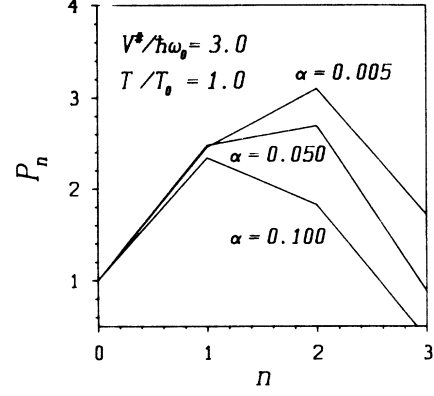


FIG. 6. Normalized thermal weights  $P_n$  ( $n=0,1,2,3$  denotes the excitation level in the system mode) for a coupled system of a harmonic plus a cubic oscillator with reduced barrier height  $V^\ddagger/\hbar\omega_0=3$ , but now the coupling strength  $\alpha$  is varied and the temperature is fixed at  $T_0$ , the bare crossover temperature.

for the uncoupled system ( $V^\ddagger/\hbar\omega_0=3$ ) at three different temperatures for four resonance states. Clearly at temperature  $T_0$  the distribution reaches a maximum around  $n=2$ , while lowering  $T$  shifts the maximum to lower  $n$ .

In Fig. 6 we show a similar plot; this time, though, the temperature is fixed at  $T_0$  [Eq. (2.14)] but the coupling parameter  $\alpha$  is varied. It is evident that increasing the coupling shifts the maximum to lower  $n$  such that the rate at the temperature  $T_0$  will be dominated by tunneling and not by thermal activation. Thus the numerical results indicate that for the present model ( $\omega_c \ll \omega_0$ ), the crossover temperature *increases* with increased dissipation, in contrast to Eq. (4.2).

This effect can be understood in terms of the sudden approximation. As already demonstrated in the preceding section, the sudden theory seems to provide a good representation of the dynamics of the model. The sudden dynamics are dominated by the normal-mode expansion around the well. Thus the imaginary frequency of the sudden barrier (at  $v'=0$ ) is  $\lambda_0$  (since the potential is cubic) and not  $\lambda_0^\ddagger$  [cf. Eq. (3.1)]; note that time has been scaled as  $1/\lambda_0$ . Therefore, the sudden theory estimate for the crossover temperature  $T_\alpha^s$ , i.e.,

$$k_B T_\alpha^s = \hbar\lambda_0 / 2\pi, \quad (4.5)$$

is *larger* than  $T_0$ , in qualitative agreement with the results presented in Fig. 6.

## V. DISCUSSION

The numerical results presented in Sec. II are a benchmark against which analytic theories of dissipative tunneling may be tested. Qualitatively we have already verified two important predictions of the instanton-based theory. We find an exponential decrease in the tunneling rate as a result of coupling to the bath. On the other hand, excitation of bath modes causes an enhancement of the tunneling rate. The dissipative, thermally averaged

canonical rate [cf. Eq. (2.13)] is, however, always smaller than the thermally averaged canonical gas-phase rate (see Table IV).

Within the range of parameters used in this study, we find that individual resonance states may be assigned according to the normal modes at the well. This enabled a well-defined evaluation of thermally averaged (with respect to the low-frequency bath mode) rates from individual resonance states of the “system” high-frequency mode. Here we found two important results:

(i) The ground-state rate with dissipation is at all temperatures below  $T_0$  lower than the uncoupled ( $\alpha=0$ ) gas-phase rate from the ground state. This is in agreement with the Euclidean temperature-dependent action of the instanton that is a positive definite function with respect to arbitrary damping.

(ii) Dissipative rates  $\Gamma_n(T)$  of excited states may be enhanced by thermal activation over the corresponding gas phase rates  $\Gamma_n$ , in agreement with a previous prediction from the sudden theory.<sup>19</sup>

We have used the numerical results to test the sudden theory of dissipative tunneling. We find excellent agreement for high barriers for which, in the gas-phase limit, the instanton estimate is good. For low barriers, the instanton result is not very precise, and the sudden theory based on it is only semiquantitative at  $T=0$  K. Even here though, the temperature effect is accurately accounted for by the sudden theory, verifying the analysis of Martinis and Grabert<sup>25</sup> in which the sudden approach is applied only to low-frequency bath excitations but not to the ground state  $T=0$  K rate.

Perhaps the most interesting result of the numerical simulation is the analysis of crossover between tunneling and thermal activation. It is “common knowledge” that macroscopic systems tend to be more classical mechanical in nature than their microscopic counterparts. The exponential decrease of tunneling rates with dissipation is a manifestation of this trend. Similarly, the predicted *decrease* of the crossover temperature [cf. Eq. (4.2)] with dissipation is consistent with this principle. In this work, we have found the opposite trend—the crossover temperature *increases* as a result of coupling. Here, dissipation enhances quantum effects, counter to usual intuition.

Is this result limited in the sense that it will disappear when we couple the system to a true continuum? What is “wrong” in the instanton-based prediction [Eq. (4.2)]? We believe that the increase in crossover temperature is

intimately connected with the validity of the sudden theory at the crossover temperature. Consider first ohmic friction. At the crossover temperature we will find excited bath modes whose frequency is identical to the system frequency and the sudden approximation is no longer valid. Here, we expect the “normal” behavior, i.e., a lower crossover temperature as a result of damping.

If the bath spectrum is such that the bath frequencies are greater than the system frequency, then we know that an adiabatic approximation is valid. In the adiabatic limit, bath excitations decrease the tunneling rate,<sup>13a</sup> and so we again expect the normal result. In other words, for “generic baths” we expect the instanton-based prediction [Eq. (4.2)] to be valid. However, if the spectral density of the bath has a cutoff frequency  $\omega_c$  which is lower than the system frequency, we expect (and have shown in this paper) that the sudden approximation will reflect the true dynamics. Analysis of the numerical results in terms of the sudden approach indicates that whenever the sudden approach is valid we should expect an increased crossover temperature as a result of coupling *irrespective* of the number of modes. With the sudden approximation, the barrier frequency is the normal mode frequency  $\lambda_0$  which is shifted to the blue for *all* baths, obeying  $\omega_c < \omega_0$ .

Why does the instanton-based analysis not lead to the same conclusion? Note that the instanton is an entity that moves around the barrier. Around  $T \sim T_0$ , the instanton is close to the top of the barrier and does not have information on the dynamics of the classically allowed region of the well. As is evident from Table I as well as from an analysis, for intermediate to strong coupling, the unstable normal mode at the barrier is virtually perpendicular to the normal mode at the well. Thus tunneling along the instanton path demands strong curvature in the classically allowed region. This curvature is not accounted for in the instanton approach.

#### ACKNOWLEDGMENTS

We thank Professor N. Moiseyev and Dr. E. Engdahl for insightful discussions on the complex scaling method and acknowledge useful discussion on matrix continued-fraction techniques with Dr. P. Jung. This work was supported by grants of the Minerva Foundation, the Albert Leimer Foundation, and the U.S. Israel Binational Science Foundation.

<sup>1</sup>R. A. Harris and L. Stodolsky, Phys. Lett. **78B**, 313 (1978); J. Chem. Phys. **74**, 2145 (1981).

<sup>2</sup>M. Simonius, Phys. Rev. Lett. **40**, 980 (1978).

<sup>3</sup>A. O. Caldeira and A. J. Leggett, Ann. Phys. (N.Y.) **149**, 374 (1983); **153**, 455(E) (1984).

<sup>4</sup>G. W. Ford, M. Kac, and P. Mazur, J. Math. Phys. **6**, 504 (1965).

<sup>5</sup>R. Zwanzig, J. Stat. **9**, 215 (1973).

<sup>6</sup>C. G. Callan and S. Coleman, Phys. Rev. D **16**, 1762 (1977).

<sup>7</sup>W. H. Miller, J. Chem. Phys. **62**, 1899 (1975).

<sup>8</sup>P. Hänggi, J. Stat. Phys. **42**, 105 (1988); Ann. N.Y. Acad. Sci. **480**, 51 (1986).

<sup>9</sup>H. Grabert, in *SQUID 85*, edited by H. D. Hahlbohm and H. Lübbig (De Gruyter, Berlin, 1985).

<sup>10</sup>H. Grabert, P. Olschowski, and U. Weiss, Phys. Rev. B **36**, 1931 (1987).

<sup>11</sup>H. Grabert, U. Weiss, and P. Hänggi, Phys. Rev. Lett. **52**, 2193 (1984).

- <sup>12</sup>R. A. Harris and R. Silbey, *J. Chem. Phys.* **83**, 1069 (1985), and references therein.
- <sup>13</sup>(a) E. Pollak, *Phys. Rev. A* **33**, 4244 (1986); (b) *Chem. Phys. Lett.* **127**, 178 (1986).
- <sup>14</sup>Yu. I. Dakhnovskii and A. A. Ovchinnikov, *Phys. Lett. A* **113**, 147 (1985).
- <sup>15</sup>P. Hänggi and W. Hontscha, *J. Chem. Phys.* **88**, 4094 (1988).
- <sup>16</sup>S. Washburn, R. A. Webb, R. F. Voss, and S. M. Faris, *Phys. Rev. Lett.* **54**, 2712 (1985); D. B. Schwartz, B. Sen, C. N. Archie, and J. E. Lukens, *ibid.* **55**, 1547 (1985); J. M. Martinis, M. H. Devoret, and J. Clarke, *ibid.* **55**, 1908 (1985); *Phys. Rev. B* **35**, 4682 (1987); A. N. Cleland, J. M. Martinis, and J. Clarke, *ibid.* **37**, 5950 (1988).
- <sup>17</sup>S. Chapman, B. C. Garrett, and W. H. Miller, *J. Chem. Phys.* **63**, 2710 (1975); T. Banks, C. M. Bender, and T. T. Wu, *Phys. Rev. D* **8**, 3346 (1973); **8**, 3366 (1973); H. J. de Vega, J. L. Gervais, and B. Sakita, *ibid.* **19**, 604 (1979); J. N. L. Connor and A. D. Smith, *Mol. Phys.* **45**, 149 (1982).
- <sup>18</sup>N. Moiseyev and J. O. Hirschfelder, *J. Chem. Phys.* **88**, 1063 (1988), and references therein.
- <sup>19</sup>A. M. Levine, W. Hontscha, and E. Pollak, *Phys. Rev. B* **40**, 2138 (1989).
- <sup>20</sup>A. M. Levine, M. Shapiro, and E. Pollak, *J. Chem. Phys.* **88**, 1959 (1988).
- <sup>21</sup>H. Risken, *The Fokker-Planck Equation*, Vol. 18 of *Springer Series in Synergetics*, edited by H. Haken (Springer-Verlag, Berlin, 1984), Chap. 9.
- <sup>22</sup>R. Yaris, J. Bendler, R. A. Lovett, C. M. Bender, and P. A. Fedders, *Phys. Rev. A* **18**, 1816 (1978).
- <sup>23</sup>U. Weiss and W. Häffner, *Phys. Rev. D* **27**, 2916 (1983).
- <sup>24</sup>P. Hänggi, U. Weiss, and P. S. Riseborough, *Phys. Rev. A* **34**, 4558 (1986).
- <sup>25</sup>J. M. Martinis and H. Grabert, *Phys. Rev. B* **38**, 237 (1988).
- <sup>26</sup>P. Hänggi, H. Grabert, G. Ingold, and U. Weiss, *Phys. Rev. Lett.* **55**, 761 (1985).